JOURNAL OF THEORETICAL
AND APPLIED MECHANICS
**64**, 1, pp. 29–44, Warsaw 2026
https://doi.org/10.15632/jtam-pl/214265

# RESEARCH ON ADAPTIVE FUZZY SLIDING MODE CONTROL WITH SWITCHING STRATEGY FOR TRAJECTORY TRACKING OF DIGITAL HYDRAULIC CYLINDER

Shouling JIANG[1*], Qi CHEN[2]

[1] *School of Computer, Heze University, Shandong, China*
[2] *Heze University Library, Heze University, Shandong, China*
*corresponding author, *jiangshouling@hezeu.edu.cn*

Aiming at the position control system of digital hydraulic cylinders with multiple nonlinear factors and coupled forces, this study proposes a switched fuzzy sliding mode adaptive control strategy (TDAFSMC). This study proposes a TDAFSMC strategy that employs fuzzy logic to approximate switching terms for chattering suppression, while utilizing a tracking differentiator to enhance dynamic response characteristics. Lyapunov theory ensures stability through adaptive weight adjustment. Simulations show 41.7 % faster response and 2.0 % lower error versus PID. With response speed error maintained below 8.0 % and tracking error under 1.0 %, they confirm the feasibility, effectiveness, and superior performance of the proposed control strategy.

**Keywords:** tracking differentiator; fuzzy control; sliding mode variable structure control; adaptive control; digital hydraulic cylinder.

Articles in JTAM are published under Creative Commons Attribution 4.0 International.
Unported License https://creativecommons.org/licenses/by/4.0/deed.en.
By submitting an article for publication, the authors consent to the grant of the said license.

## 1. Introduction

Compared with traditional hydraulic transmission systems and electro-hydraulic servo control systems, digital hydraulic cylinders have gained widespread industrial applications due to their structural simplicity, precise control capability, and relatively low cost. However, the inherent nonlinearity, time-varying characteristics, and strong coupling effects of digital hydraulic cylinders have made their precise and stable control a key focus in both academic research and industrial practice (Qi *et al.*, 2024; Zhang *et al.*, 2025; Wang *et al.*, 2019). While conventional PID or single-loop control strategies offer simplicity in implementation, they often fail to meet the requirements for high precision and rapid response when dealing with complex nonlinear systems. Consequently, the development of advanced control strategies to enhance the positioning accuracy and operational stability of digital hydraulic cylinders has emerged as a critical challenge demanding immediate solutions.

Significant research efforts have been made by scholars worldwide to enhance the performance of electro-hydraulic servo position control systems. Gao *et al.* (2023) applied digital hydraulic cylinders to semi-active suspension systems, designing a fuzzy control-based multi-mode switching control strategy for suspension damping. This control strategy demonstrates enhanced vibration attenuation performance and contributes to improved ride comfort in vehicles. Yu *et al.* (2024) introduced a novel integrated robust control strategy that simultaneously improved system response speed, effectively suppressed system uncertainties, and enhanced high-frequency tracking performance. In addressing the nonlinearities and uncertainties inherent in hydraulic systems, He *et al.* (2023) proposed a hybrid SAC-PID control strategy. This approach employs the soft-actor critic (SAC) algorithm to dynamically adapt control parameters based on real-time system states, thereby enhancing the system's robustness. However, the reinforcement

learning framework necessitates substantial computational resources, while the initial phase of parameter tuning and optimization presents significant complexity. Liu *et al.* (2022a) proposed a self-tuning fuzzy PID positioning controller based on particle swarm optimization (PSO), which optimizes control parameters through real-time adjustment of quantization and scaling factors, thereby significantly improving the system's tracking accuracy. However, the iterative optimization process of the PSO algorithm requires considerable computational effort, which may compromise the real-time control performance. Zhang *et al.* (2024) presented an enhanced beetle antennae search (BAS) algorithm-optimized fuzzy PID controller for improving electromechanical actuator performance. The proposed control scheme demonstrates superior stability across various signal response tests, achieving significant performance enhancement. Guo *et al.* (2022) developed a Kalman-GA-optimized PID controller to improve response time, accuracy, and anti-interference in position control. Results show enhanced performance versus traditional methods, though it requires accurate modeling and lacks online self-tuning. Liu *et al.* (2022b) investigated a variable-domain fuzzy PID static compensation algorithm to address nonlinearities induced by valve dead-zone and friction in electro-hydraulic proportional servo systems. Simulation results demonstrate significant improvement in system response speed, though with relatively modest enhancement in control accuracy.

While the aforementioned control methods have improved system performance to varying degrees, the enhancement in system responsiveness remains relatively limited. To address this challenge, sliding mode variable structure control (SMC) has emerged as a prominent approach for response improvement. Đào *et al.* (2023) proposed a sliding mode controller incorporating PID direct parameter adjustment (SMCPID) for hydraulic cylinder systems. While this control strategy effectively mitigates chattering, the inherent high-frequency switching characteristics of sliding mode control may still induce actuator wear, potentially compromising long-term reliability. Sun *et al.* (2022) addressed the issues of prolonged reaching time to sliding surfaces and high-frequency chattering by proposing an adaptive reaching law-based control method with an auxiliary sub-reaching law. Simulation results on electro-hydraulic position servo systems demonstrate improved robustness, though minor chattering persists. Yang *et al.* (2019) presented an enhanced adaptive sliding mode control scheme for electro-hydraulic position servo systems exhibiting parameter uncertainties and bounded disturbances. The proposed approach employs a saturation function to replace the adjustable signum gain coefficient, effectively mitigating control chattering. Comparative experimental results conclusively demonstrate the scheme's efficacy. Ji *et al.* (2021) proposed a backstepping-based adaptive sliding mode controller for electro-hydraulic systems with parametric uncertainties and random disturbances. While improving system performance, the backstepping approach requires iterative virtual control design and Lyapunov functions, potentially causing "complexity explosion" in high-order systems. Ghani *et al.* (2022) proposed a fuzzy sliding mode method for trajectory tracking in electro-hydrostatic actuators (EHA). Experimental results demonstrate superior effectiveness, though simultaneous tuning of fuzzy membership functions, sliding surface parameters, and switching gains increases implementation complexity. Zhang *et al.* (2022) presented a variable-approaching-law fuzzy sliding mode control (FSMC) strategy to enhance the trajectory tracking performance of omni-directional wheeled robotic mobile platforms. Simulation experiments validate the method's effectiveness in achieving robust dynamic stability. Dang *et al.* (2021) addressed tracking accuracy degradation in hydraulic servo systems caused by nonlinear friction and unstructured uncertainties. An improved adaptive backstepping integral sliding mode control with incomplete differentiation (ID-BIABISMC) is proposed, demonstrating superior tracking precision in comparative experiments.

Li and Cao (2021) proposed a tracking differentiator combined with adaptive nonlinear PID (TD-NPID) to address low synchronization accuracy in multi-cylinder cooperative propulsion control of shield hydraulic systems under heavy load variations, demonstrating effective improvement in system synchronization performance. To achieve precise tracking control of the voice

coil actuator fast steering mirror (VCA-FSM) with large measurement noise, a nonsingular terminal sliding mode (NTSMC) method based on a differentiator (TD) is proposed. Experimental results from the hardware-in-the-loop (HIL) test bench validate the method's effectiveness in meeting both dynamic response and steady-state accuracy requirements (Li *et al.*, 2023).

The aforementioned studies have systematically investigated the performance of electro-hydraulic servo systems through numerical simulations and experimental validations, establishing a solid theoretical foundation. These research efforts reveal that while sliding mode variable structure control effectively enhances system rapidity, increasing switching gains inevitably induces chattering phenomena. To address this limitation, fuzzy control is employed to approximate the switching term, thereby achieving term continuity and significantly mitigating chattering effects. Furthermore, the incorporation of a TD provides comprehensive dynamic characteristics for the controller. Building upon these insights, this paper proposes a novel TD-based switched fuzzy sliding mode adaptive control (TDAFSMC) strategy that synergistically integrates these three control methodologies. The fuzzy adaptive law is rigorously derived through Lyapunov stability theory, with adaptive weight adjustments ensuring both stability and convergence of the entire closed-loop system. For a comprehensive evaluation, MATLAB simulation software is utilized to model and analyze the performance of digital hydraulic cylinder positioning systems under the proposed TDAFSMC strategy. Additionally, an experimental testbed is constructed to empirically validate the control strategy's effectiveness under practical operating conditions.

## 2. Double-loop digital hydraulic cylinder state space model

The double-loop digital hydraulic cylinder system primarily consists of five key components: a servo motor, coupling mechanism, four-way spool valve, internal indirect feedback mechanism, and a conventional hydraulic cylinder. The internal indirect feedback mechanism comprises a ball screw assembly and spool feedback linkage. The thrust bearing tightly presses the ball screw against the cylinder cover, allowing the screw only one rotational degree of freedom. Both the piston and the screw nut are fixed in position. A threaded piston pair is formed between the screw and piston, while the other end of the screw is threadedly connected to the right end of the spool, forming a threaded spool pair. The right end of the servo motor is connected to the left end of the spool through the coupling. The spool has only one axial degree of freedom relative to the output shaft of the servo motor, forming a sliding spool pair. The schematic diagram of this structural principle is shown in Fig. 1.

The operational principle of the system is as follows: When the command signal is zero, the zero-opening four-way spool valve remains stationary, keeping the hydraulic cylinder piston rod at rest. With a positive command signal, a potential difference is generated to drive the servo motor, causing the spool to move leftward and open the valve port. Under the high-pressure oil, the piston moves leftward while the ball screw rotates circumferentially in the opposite direction to the servo motor. This screw rotation drives the spool rightward to close the valve port until the deviation reaches zero. A negative command signal triggers the reverse process. Thus, the position of the digital hydraulic cylinder changes according to the command signal variations. The structural diagram of this double-loop digital hydraulic cylinder position control system is shown in Fig. 2.

Jiang *et al.* (2022) provided a comprehensive theoretical analysis of the digital hydraulic cylinder's working principle and established an enhanced mathematical model that incorporates the dynamics of both the digital spool valve and feedback mechanism. This advanced model integrates critical nonlinear factors including transmission backlash, spool valve radial leakage, and LuGre friction characteristics, thereby achieving more accurate representation of actual system behavior. Building upon this established theoretical foundation, the present study directly presents the consolidated nonlinear state-space model without redundant elaboration.

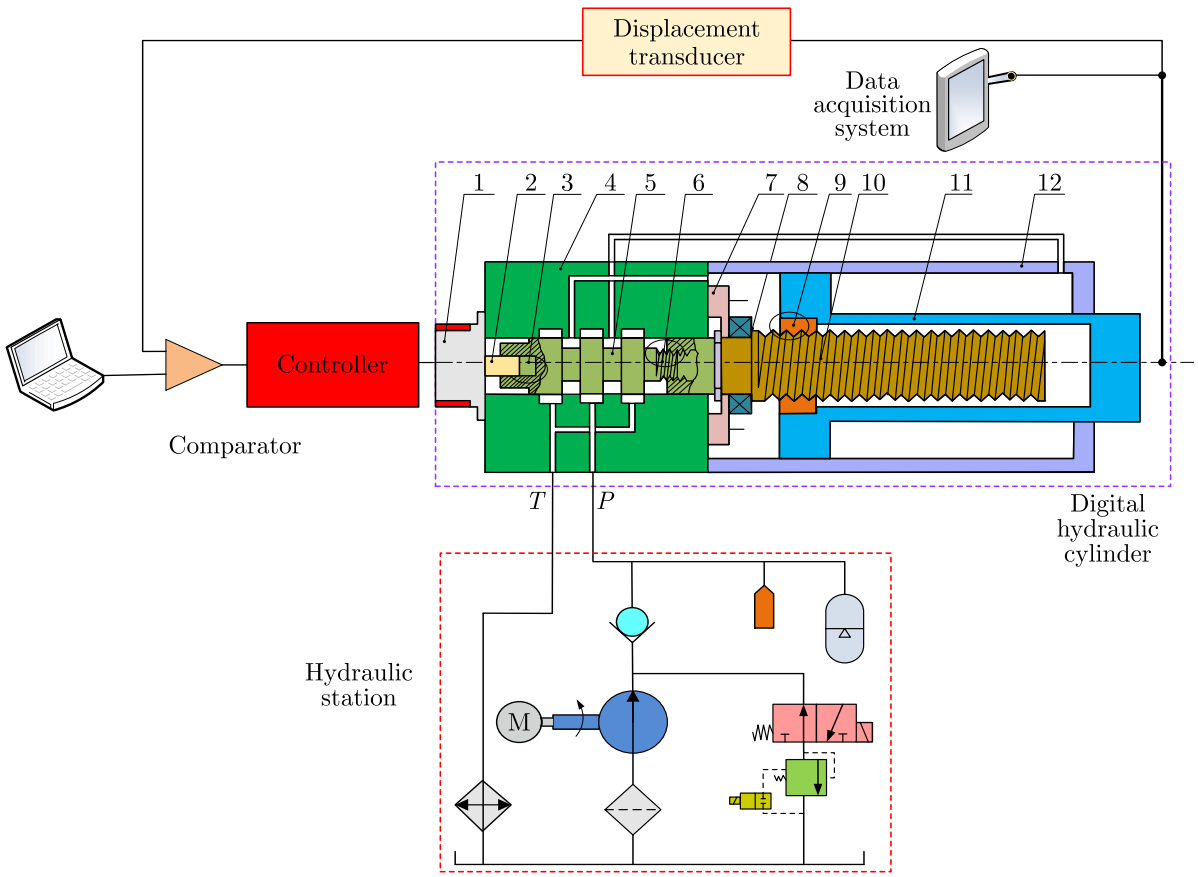


Fig. 1. Working principle diagram of digital hydraulic cylinder: 1 – servo motor; 2 – coupler, 3 – valve spool sliding pair; 4 – valve body; 5 – spool; 6 – spool thread pair; 7 – fixed sleeve; 8 – thrust bearing; 9 – piston thread pair; 10 – ball screw; 11 – piston rod; 12 – cylinder body.

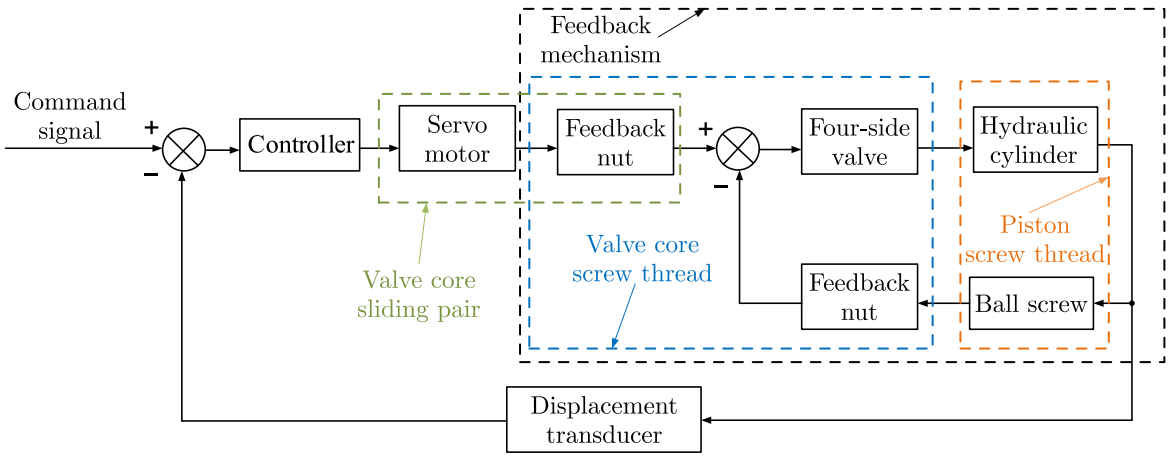


Fig. 2. Double closed-loop digital hydraulic cylinder position control system structure diagram.

The system control input is $u_q$, the output piston rod displacement is $y = x_1 = x_p$, the system state variable is $x$:

$$x = [x_1,\, x_2,\, x_3,\, x_4,\, x_5,\, x_6,\, x_7,\, x_8,\, x_9,\, x_{10},\, x_{11},\, x_{12},\, x_{13},\, x_{14}]^{\mathrm{T}}$$
$$= \left[x_p,\, \dot{x}_p,\, P_1,\, P_2,\, x_v,\, \dot{x}_v,\, \theta_s,\, \dot{\theta}_s,\, \theta_v,\, \dot{\theta}_v,\, \theta_\tau,\, \dot{\theta}_\tau,\, z, i_q\right]^{\mathrm{T}}. \tag{2.1}$$

Therefore, the state equation of the system can be expressed as

$$\begin{cases} \dot{x}_1 = x_2, \\ \dot{x}_2 = \begin{bmatrix} A_1\left(x_3 - mx_4\right) - F_{np}\cos\alpha_p - F_{tp}\sin\alpha_p - \left(k_1x_1 + k_3x_1^3\right) \\ -\sigma_0x_{13} + \sigma_1\dfrac{|x_2|}{g\left(x_2\right)}x_{14} + \left(\sigma_2 - \sigma_1\right)x_2 \end{bmatrix} \Big/ M_t + w_1, \\ \dot{x}_3 = \left[Q_1 - A_1x_2\right]\beta_e/(V_{01} + A_1x_1) + w_2, \\ \dot{x}_4 = \left[-Q_2 - A_2x_2\right]\beta_e/(V_{02} - A_2x_1) + w_3, \\ \dot{x}_5 = x_6, \\ \dot{x}_6 = \left[F_{nv}\cos\alpha_v - F_{tv}\sin\alpha_v - F_{yd} - B_{vp}x_6 - F_{tg} - F_{fv}\right]/m_v, \\ \dot{x}_7 = x_8, \\ \dot{x}_8 = \left[r_{vs}F_{nv}\sin\alpha_v + r_{vs}F_{tv}\cos\alpha_v + r_{ps}F_{np}\sin\alpha_p - r_{ps}F_{tp}\cos\alpha_p - T_{fs} - B_sx_8\right]/J_s, \\ \dot{x}_9 = x_{10}, \\ \dot{x}_{10} = \left[\mathrm{r}_\tau F_{ng} - r_sF_{nv}\sin\alpha_v - r_sF_{tv}\cos\alpha_v - B_{vz}x_{10} - T_{fv}\right]/J_v, \\ \dot{x}_{11} = x_{12}, \\ \dot{x}_{12} = \left[k_tx_{14} - B_2x_{12} - r_\tau F_{ng}\right]/J, \\ \dot{x}_{13} = x_2 - \sigma_0\dfrac{|\dot{x}_2|}{F_c + \left(F_{sc} - F_c\right)e^{-\left(x_2/v_{sk}\right)^2}}x_{13}, \\ \dot{x}_{14} = \left[u_q - Rx_{14} - k_ex_{12}\right]/L_0, \end{cases} \tag{2.2}$$

where

$$w_1 = -F_L/M_t, \quad w_2 = \frac{\left[-C_0x_3 - C_1\left(x_3 - x_4\right)\right]\beta_e}{V_{01} + A_1x_1}, \quad w_3 = \frac{\left[-C_0x_4 + C_1\left(x_3 - x_4\right)\right]\beta_e}{V_{02} - A_2x_1}.$$

Let us consider the hydraulic cylinder load force and leakage as disturbances in the system, namely

$$\begin{cases} w_2 \le \dfrac{\beta_eP_s\left(C_1 + C_0\right)}{|V_1|_{\min}}, \\ w_3 \le \dfrac{\beta_eP_s\left(C_1 + C_0\right)}{|V_2|_{\min}}. \end{cases} \tag{2.3}$$

Therefore, the disturbances $w_1$, $w_2$, and $w_3$ are bounded:

$$w = \begin{bmatrix} 0 & w_1 & w_2 & w_3 & 0 & \dots & 0 \end{bmatrix}_{1\times 14}. \tag{2.4}$$

And the system state space expression is

$$\begin{cases} \dot{x} = f(x) + g(x)u + p(x)w, \\ z = h(x)x. \end{cases} \tag{2.5}$$

In formula (2.5):

$$
f(x)=\begin{cases}
\dot{x}_1=x_2,\\
\dot{x}_2=\left[\begin{array}{r} A_1\left(x_3-mx_4\right)-F_{np}\cos\alpha_p-F_{tp}\sin\alpha_p-\left(k_1x_1+k_3x_1^3\right)\\ -\sigma_0x_{13}+\sigma_1\dfrac{|x_2|}{g\left(x_2\right)}x_{14}+\left(\sigma_2-\sigma_1\right)x_2\end{array}\right]\Big/M_t,\\
\dot{x}_3=\left[Q_1-A_1x_2\right]\beta_e/(V_{01}+A_1x_1),\\
\dot{x}_4=\left[-Q_2-A_2x_2\right]\beta_e/(V_{02}-A_2x_1),\\
\dot{x}_5=x_6,\\
\dot{x}_6=\left[F_{nv}\cos\alpha_v-F_{tv}\sin\alpha_v-F_{yd}-B_{vp}x_6-F_{tg}-F_{fv}\right]/m_v,\\
\dot{x}_7=x_8,\\
\dot{x}_8=\left[\begin{array}{r} r_{vs}F_{nv}\sin\alpha_v+r_{vs}F_{tv}\cos\alpha_v+r_{ps}F_{np}\sin\alpha_p\\ -r_{ps}F_{tp}\cos\alpha_p-T_{fs}-B_sx_8\end{array}\right]\Big/J_s,\\
\dot{x}_9=x_{10},\\
\dot{x}_{10}=\left[\mathrm{r}_\tau F_{ng}-r_sF_{nv}\sin\alpha_v-r_sF_{tv}\cos\alpha_v-B_{vz}x_{10}-T_{fv}\right]/J_v,\\
\dot{x}_{11}=x_{12},\\
\dot{x}_{12}=\left[k_tx_{14}-B_2x_{12}-r_\tau F_{ng}\right]/J,\\
\dot{x}_{13}=x_2-\sigma_0\dfrac{|\dot{x}_2|}{F_c+\left(F_{sc}-F_c\right)e^{-\left(x_2/v_{sk}\right)^2}}x_{13},\\
\dot{x}_{14}=\left[-Rx_{14}-k_ex_{12}\right]/L_0,
\end{cases}
\tag{2.6}
$$

$$
\begin{cases}
g(x)=\left[\begin{array}{ccccc}0 & \ldots & 0 & 0 & 1\end{array}\right]_{1\times14}^{\mathrm{T}},\\
p(x)=\left[\begin{array}{ccccccc}0 & 1 & 1 & 1 & 0 & \ldots & 0\end{array}\right]_{1\times14}^{\mathrm{T}},\\
h(x)=\left[\begin{array}{ccccc}1 & 0 & 0 & \ldots & 0\end{array}\right]_{1\times14}.
\end{cases}
\tag{2.7}
$$

## 3. Design of the TDAFSMC controller

TD is essentially a signal processing technique that filters the input signal and extracts its derivative. Particularly when the input signal undergoes abrupt changes, the TD can provide a smooth input signal for the controller. Meanwhile, its filtering capability mitigates the impact of sudden signal variations, preventing system overshoot. This effectively resolves the inherent conflict between "rapid response" and "overshoot", thereby enhancing system stability. The TD can achieve the dynamic performance metrics of closed-loop systems, ensuring high-quality real-time tracking curves for the system.

In this study, the digital hydraulic cylinder is modeled as a second-order system. For continuously differentiable input signals, a conventional second-order TD in cascade configuration would

suffice. However, when the input signal is a step function, its derivative theoretically approaches infinity. To address this fundamental limitation, a third-order TD is proposed in this work.

The third-order TD formulation constructed using the inverse hyperbolic sine function *arsh* is presented as follows:

$$\begin{cases} \dot{v}_1 = v_2, \\ \dot{v}_2 = v_3, \\ \dot{v}_3 = R^3 \left\{ -a_1 \mathrm{arsh}\left[b_1\left(v_1(t) - r(t)\right)\right] - a_2 \mathrm{arsh}\left[b_2 v_2(t)/R\right] - a_3 \mathrm{arsh}\left[b_3 v_3(t)/R^2\right] \right\}. \end{cases} \tag{3.1}$$

In formula (3.1), $r(t)$ represents the input signal, and all parameters are positive constants.

For any bounded integrable input signal $r(t)$, given a sufficiently large parameter $R$, the solution of Eq. (3.1) can asymptotically converge to $r(t)$ within arbitrary finite time, yielding outputs $v_2(t) = \dot{r}(t)$ and $v_3(t) = \ddot{r}(t)$. The proposed TD demonstrates superior differential tracking capability while effectively suppressing derivative noise amplification, making it widely applicable in engineering implementations.

To enhance the system's rapid response capability, this paper employs sliding mode variable structure control. However, increasing the switching gain may induce chattering phenomena. To address this issue, fuzzy control is adopted to approximate the switching term, thereby achieving term continuity and effectively mitigating chattering. Below we present the design of a fuzzy sliding mode adaptive controller.

The switching function is formally defined as follows:

$$s(x,t) = k_1 e + k_2 \dot{e} + ... + k_{n-1} e^{(n-1)} + e^{(n-1)} = ke, \tag{3.2}$$

where the matrices $e = x - x_d = \left(e, \dot{e}, ..., e^{(n-1)}\right)^{\mathrm{T}}$ and $k_1, k_2, ..., k_{n-1}$ satisfy the Hurwitz polynomial condition.

The sliding mode control law is designed as follows:

$$u(t) = \frac{1}{g(x,t)} \left( -f(x,t) - \sum_{i=1}^{n-1} k_i e^{(i)} + x_d^{(n)} - u_{sw} \right). \tag{3.3}$$

In formula (3.3), $u_{sw} = \eta \,\mathrm{sgn}\,(s)$, $\eta \geq D$. Thus:

$$\begin{aligned} \dot{s}(x,t) &= \sum_{i=1}^{n-1} k_i e^{(i)} + e^{(n)} = \sum_{i=1}^{n-1} k_i e^{(i)} + x^{(n)} - x_d^{(n)} \\ &= \sum_{i=1}^{n-1} k_i e^{(i)} + f(x,t) + g(x,t)u(t) + d(t) - x_d^{(n)}. \end{aligned} \tag{3.4}$$

Substituting formula (2.5) and formula (3.3) yields:

$$s(x,t) \cdot \dot{s}(x,t) = ds - \eta\,|s| \leq 0. \tag{3.5}$$

When the upper bounds of $f$, $g$, and d are unknown, the control law (3.3) becomes inapplicable. To address this limitation, fuzzy systems $\widehat{f}$, $\widehat{g}$, and $\widehat{h}$ are employed to approximate $f$, $g$, and $\eta\,\mathrm{sgn}\,(s)$, respectively.

The fuzzy systems are constructed using a product inference engine, singleton fuzzifier, and center-average de-fuzzifier, with their respective outputs designated as $\widehat{f}$, $\widehat{g}$, and $\widehat{h}$, whereby the control law is consequently modified to:

$$u(t) = \frac{1}{\widehat{g}(x,t)} \left( -\widehat{f}(x,t) - \sum_{i=1}^{n-1} k_i e^{(i)} + x_d^{(n)} - \widehat{h}(s) \right), \tag{3.6}$$

$$\begin{cases} \widehat{f}\left(x|\,\theta_f\right) = \theta_f^T \xi(x), \\ \widehat{g}\left(x|\,\theta_g\right) = \theta_g^T \xi(x), \\ \widehat{h}\left(s|\,\theta_h\right) = \theta_h^T \phi(s), \end{cases} \tag{3.7}$$

where $\widehat{f}\left(x|\,\theta_f\right)$, $\widehat{g}\left(x|\,\theta_g\right)$, and $\widehat{h}\left(s|\,\theta_h\right)$ denote the outputs of the fuzzy systems, $\xi(x)$ and $\phi(s)$ represent fuzzy vectors, while $\theta_f^T$, $\theta_g^T$, and $\theta_h^T$ are dynamically adjusted according to the adaptive laws;

$$\widehat{h}\left(x|\,\theta_h^*\right) = \eta_\Delta \mathrm{sgn}\left(s\right), \tag{3.8}$$

$$\eta_\Delta = D + \eta \qquad \eta \geq 0, \tag{3.9}$$

$$|d| \leq D. \tag{3.10}$$

The adaptive laws are designed as follows:

$$\begin{cases} \dot{\theta}_f = r_1 s \xi(x), \\ \dot{\theta}_g = r_2 s \xi(x) u, \\ \dot{\theta}_h = r_3 s \phi(s). \end{cases} \tag{3.11}$$

Subsequently, the convergence proof of the controller is established, where the optimal parameters are defined as

$$\theta_f^* = \arg \min_{\theta_f \in \Omega_f} \left[ \sup \left| \widehat{f}\left( x| \underset{x \in R^n}{\theta_f} \right) - f(x,t) \right| \right], \tag{3.12}$$

$$\theta_g^* = \arg \min_{\theta_g \in \Omega_g} \left[ \sup \left| \widehat{g}\left( x| \underset{x \in R^n}{\theta_g} \right) - g(x,t) \right| \right], \tag{3.13}$$

$$\theta_h^* = \arg \min_{\theta_h \in \Omega_h} \left[ \sup \left| \widehat{h}\left( s| \underset{x \in R^n}{\theta_h} \right) - u_{sw} \right| \right], \tag{3.14}$$

where $\Omega_f$, $\Omega_g$, and $\Omega_h$ denote the sets of $\theta_f$, $\theta_g$, and $\theta_h$, respectively.

The minimum approximation error is defined as

$$\omega = f(x,t) - \widehat{f}\left(x|\,\theta_f^*\right) + \left(g(x,t) - \widehat{g}\left(x|\,\theta_g^*\right)\right) u, \tag{3.15}$$

where $|\omega| \leq \omega_{\max}$.

Substituting the control law (3.6) yields:

$$\begin{aligned} \dot{s}(x,t) &= \sum_{i=1}^{n-1} k_i e^{(i)} + x^{(n)} - x_d^{(n)} \\ &= \sum_{i=1}^{n-1} k_i e^{(i)} + f(x,t) + g(x,t)u(t) + d(t) - x_d^{(n)} \\ &= \sum_{i=1}^{n-1} k_i e^{(i)} + f(x,t) + \widehat{g}(x,t)u(t) + \left(g(x,t) - \widehat{g}(x,t)\right) u + d(t) - x_d^{(n)} \\ &= f(x,t) - \widehat{f}(x,t) - \widehat{h}\left(s|\,\theta_h\right) + \left(g(x,t) - \widehat{g}(x,t)\right) u + d(t) \\ &= \widehat{f}\left(x|\,\theta_f^*\right) - \widehat{f}(x,t) - \widehat{h}\left(s|\,\theta_h\right) + \left(\widehat{g}\left(x|\,\theta_g^*\right) - \widehat{g}(x,t)\right) u + d(t) + \omega - \widehat{h}\left(s|\,\theta_h^*\right) \\ &= \varphi_f^T \xi(x) + \varphi_g^T \xi\left(x\right) u(t) + \varphi_h^T \phi(s) + d\left(t\right) + \omega - \widehat{h}\left(s|\,\theta_h^*\right), \end{aligned} \tag{3.16}$$

where $\varphi_f = \theta_f^* - \theta_f$, $\varphi_g = \theta_g^* - \theta_g$, $\varphi_h = \theta_h^* - \theta_h$.

The Lyapunov function candidate is defined as

$$V = \frac{1}{2}\left(s^2 + \frac{1}{r_1}\varphi_f^T\varphi_f + \frac{1}{r_2}\varphi_g^T\varphi_g + \frac{1}{r_3}\varphi_h^T\varphi_h\right), \tag{3.17}$$

where $r_1$, $r_2$, and $r_3$ are positive constants. Therefore:

$$\begin{aligned}
\dot{V} &= s\dot{s} + \frac{1}{r_1}\varphi_f^T\dot{\varphi}_f\frac{1}{r_2}\varphi_g^T\dot{\varphi}_g + \frac{1}{r_3}\varphi_h^T\dot{\varphi}_h \\
&= s\left(\varphi_f^T\xi(x) + \varphi_g^T\xi(x)u(t) + \varphi_h^T\phi(s) + d(t) + \omega - \widehat{h}\left(s|\,\theta_h^*\right)\right) \\
&\quad + \frac{1}{r_1}\varphi_f^T\dot{\varphi}_f + \frac{1}{r_2}\varphi_g^T\dot{\varphi}_g + \frac{1}{r_3}\varphi_h^T\dot{\varphi}_h \\
&= s\varphi_f^T\xi(x) + \frac{1}{r_1}\varphi_f^T\dot{\varphi}_f + s\varphi_g^T\xi(x)u(t) + \frac{1}{r_2}\varphi_g^T\dot{\varphi}_g + s\varphi_h^T\phi(s) \\
&\quad + \frac{1}{r_3}\varphi_h^T\dot{\varphi}_h + s\left(d(t) - \widehat{h}\left(s|\,\theta_h^*\right)\right) + s\omega.
\end{aligned} \tag{3.18}$$

Given $\widehat{h}\left(s|\,\theta_h^*\right) = \eta_\Delta \mathrm{sgn}\left(s\right)$, it follows that:

$$\begin{aligned}
\dot{V} &= \frac{1}{r_1}\varphi_f^T\left(r_1 s\xi(x) + \dot{\varphi}_f\right) + \frac{1}{r_2}\varphi_g^T\left(r_2 s\xi(x)u(t) + \dot{\varphi}_g\right) \\
&\quad + \frac{1}{r_3}\varphi_h^T\left(r_3 s\varphi(s) + \dot{\varphi}_h\right) + sd(t) + s\omega - \left(D + \eta\right)|s| \\
&= sd(t) + s\omega - \left(D + \eta\right)|s|,
\end{aligned} \tag{3.19}$$

where $\dot{\varphi}_f = -\dot{\theta}_f$, $\dot{\varphi}_g = -\dot{\theta}_g$, $\dot{\varphi}_h = -\dot{\theta}_h$.

Substituting the adaptive law (3.11) into the preceding equation yields:

$$\dot{V} \leq s\omega - \eta\,|s|\,. \tag{3.20}$$

Based on fuzzy approximation theory, the adaptive fuzzy system can achieve an arbitrarily small approximation error $\omega$. Consequently, by selecting a sufficiently large parameter $\eta$, the stability condition $\dot{V} \leq 0$ can be guaranteed.

When $\dot{V} \equiv 0$ holds and $s \equiv 0$ is satisfied, then according to LaSalle's invariance principle, $t \to \infty$ implies $s \to 0$.

## 4. Simulation studies

This paper conducts simulation analysis of the proposed adaptive robust control strategy in MATLAB/Simulink environment. The hydraulic system's mathematical model is implemented using S-function based on formula (2.4), while the nonlinear controller is constructed according to formula (3.6). Simultaneously, online estimation of uncertain system parameters is achieved through formula (3.8). The complete control system architecture is illustrated in Fig. 3, where the structural parameters of the digital hydraulic cylinder follow Table 1 in (Jiang *et al.*, 2022).

To verify the control performance of the proposed TDAFSMC strategy, comprehensive tracking tests were conducted using step, sinusoidal, and composite (ramp-step hybrid) reference signals to analyze the system's tracking performance under different control strategies, where the PID controller parameters were set as $k_p = 10\,000$, $k_i = 600$, $k_d = 1000$, with a filter coefficient $N = 1000$. The TDAFSMC controller parameters were set as $r_1 = 50$, $r_2 = 1$, $r_3 = 10$, $k_1 = 35$, $\theta_f^T = 0.1$, $\theta_g^T = 0.1$, and $\theta_h^T = 0.1$, with five Gaussian membership functions employed for

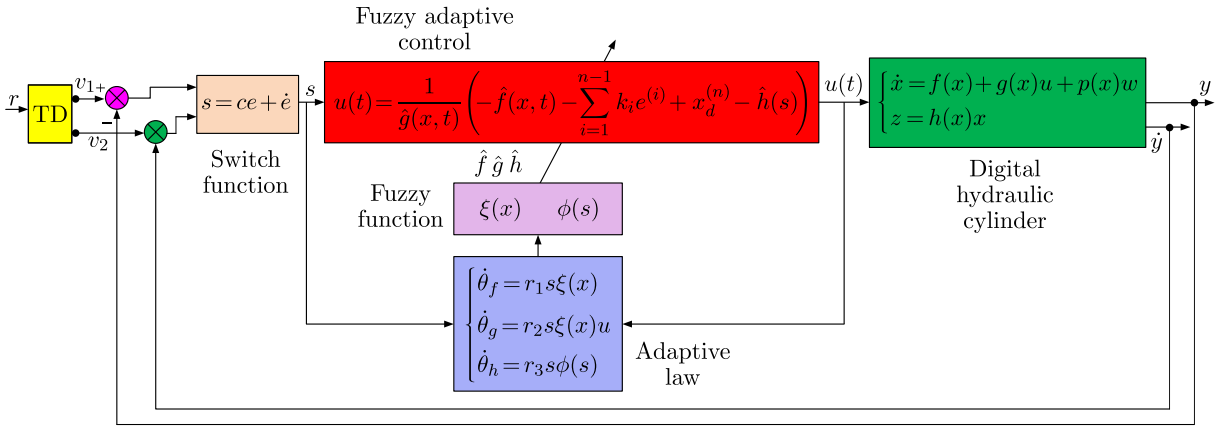


Fig. 3. Structure diagram of the digital hydraulic cylinder position control system based on TDAFSMC.

fuzzification: $\mu_{NM}(x_i) = \exp[-((x_i + \pi/6)/(\pi/24))^2]$, $\mu_{NS}(x_i) = \exp[-((x_i + \pi/12)/(\pi/24))^2]$, $\mu_Z(x_i) = \exp[-(x_i/(\pi/24))^2]$, $\mu_{PS}(x_i) = \exp[-((x_i - \pi/12)/(\pi/24))^2]$, $\mu_{PM}(x_i) = \exp[-((x_i - \pi/6)/(\pi/24))^2]$, resulting in 25 fuzzy rules each for approximating $f$ and $g$. The switching function $s(t)$ utilized sigmoidal membership functions defined as $\mu_N(s) = 1/[1 + \exp(5(s + 3)]$, $\mu_Z(s) = \exp(-s^2)$ and $\mu_P(s) = 1/[1 + \exp(5(s - 3)])$.

As shown in Fig. 4, the system's positional displacement and tracking error curves are presented for a step reference signal with a 40 mm final magnitude initiated at $t = 1$ s.

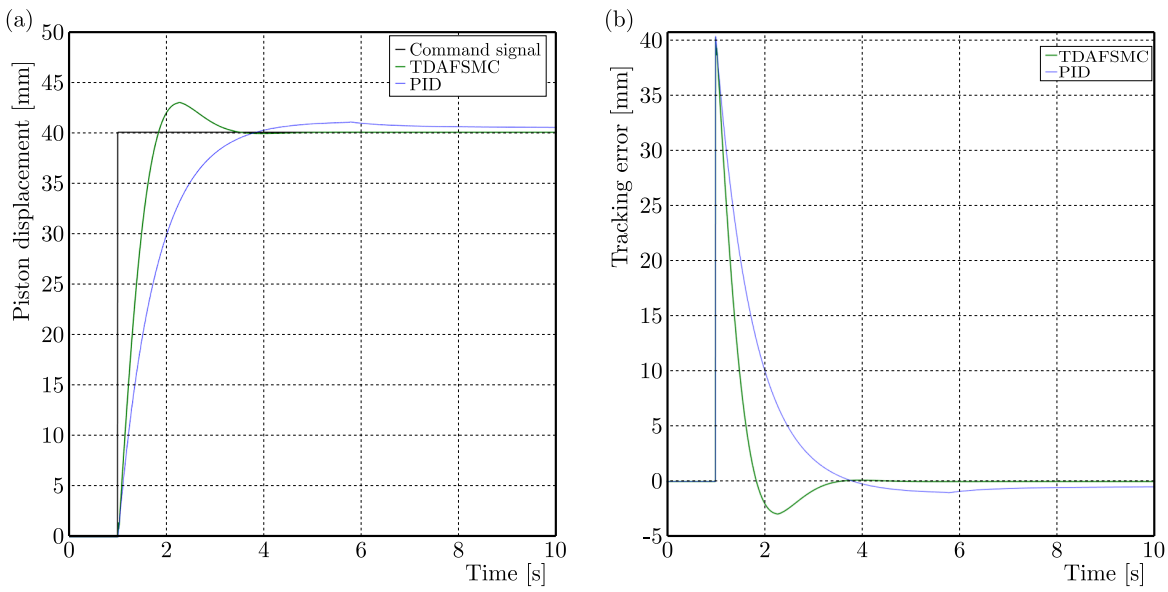


Fig. 4. Piston displacement and error curves: (a) piston displacement curve; (b) tracking error curves.

As evidenced by Fig. 4a, the PID-controlled system achieves the steady state at approximately 6 s with a residual error of 0.8 mm, whereas the proposed TDAFSMC strategy reaches the steady state in 3.5 s with near-zero error, demonstrating a 41.7 % improvement in response speed and 2.0 % enhancement in steady-state accuracy. Comparative analysis reveals that conventional PID control exhibits significant tracking errors and sluggish dynamics under nonlinear coupling forces, while the developed TDAFSMC method simultaneously achieves superior precision and faster transient response.

Figure 5 presents the system's positional tracking performance and corresponding error curves when subjected to a sinusoidal reference trajectory of $20\sin(t)$ mm, thereby demonstrating the controller's ability to manage periodic excitations.

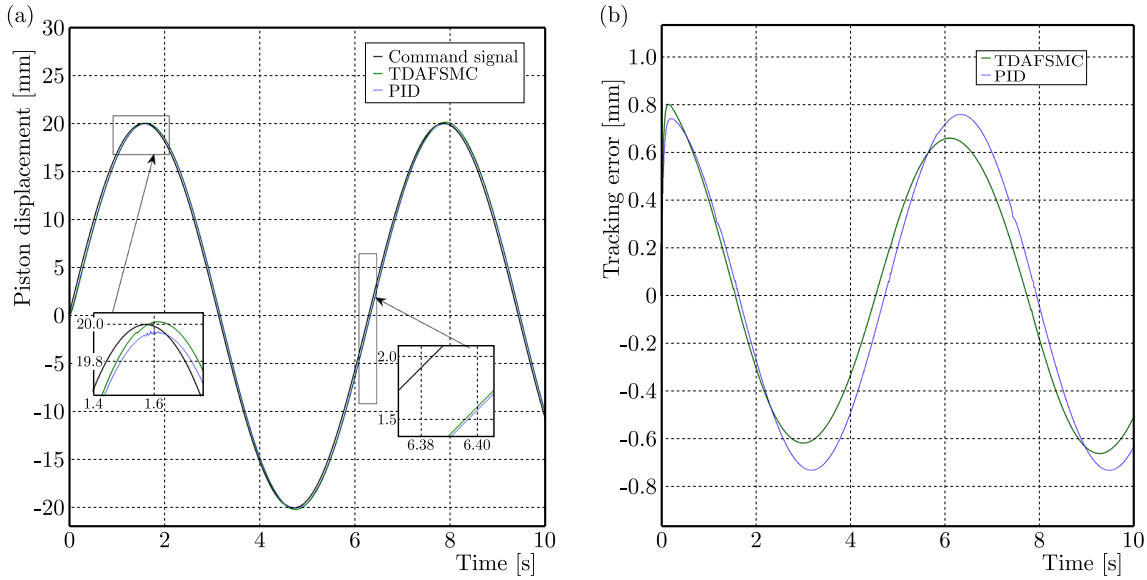


Fig. 5. Piston displacement and error curves: (a) piston displacement curve; (b) tracking error curves.

As demonstrated in Fig. 5, the tracking error under conventional PID control is confined to −0.75 mm–0.8 mm, whereas the proposed TDAFSMC strategy reduces this range to −0.6 mm–0.75 mm, achieving a measurable improvement in tracking precision. The magnified view in Fig. 5a reveals a phase lag of approximately 0.22 s for PID control throughout the simulation cycle, compared to 0.5 s for TDAFSMC. These results indicate that while traditional PID control struggles to compensate for nonlinearities such as backlash effects, the developed TDAFSMC controller effectively incorporates the digital hydraulic cylinder's nonlinear characteristics through a composite sliding-mode and fuzzy control architecture. This adaptive mechanism actively compensates for nonlinear disturbances within the control law, thereby significantly enhancing the hydraulic system's tracking performance.

The given composite signal period is 6 s, the displacement of 0 s–1 s is 0, 1 s–2 s stretches out at a slope of 40 mm/s, 2 s–4 s remains unchanged, 4 s–5 s retracts at a slope of −40 mm/s, and 5 s–6 s remains unchanged.

Figure 6 demonstrates the piston displacement curves and tracking error curves under both PID and TDAFSMC control strategies when following the custom reference signal. During the

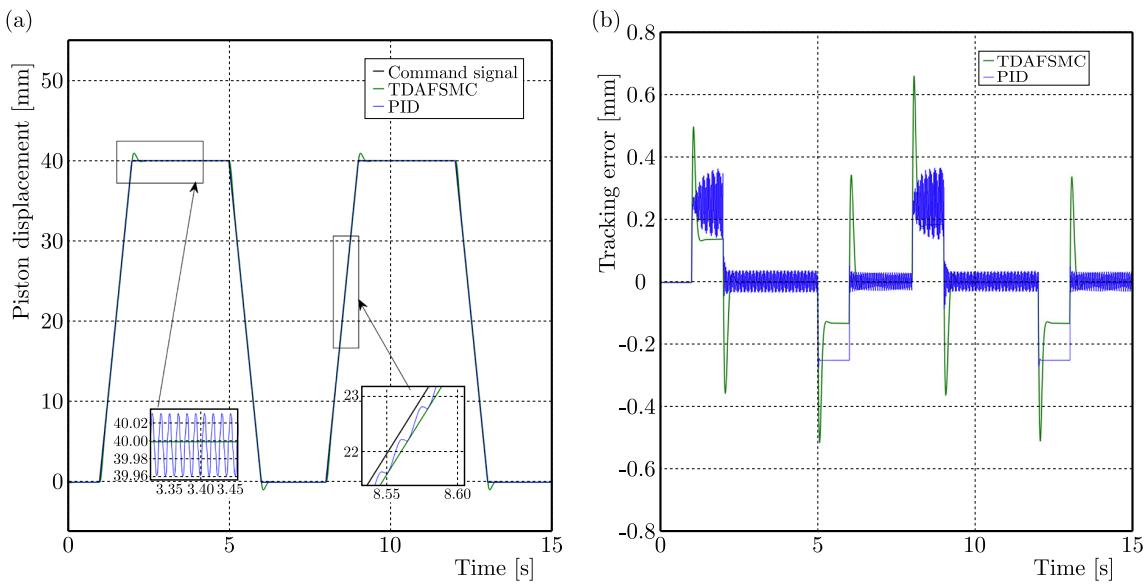


Fig. 6. Piston displacement and error curves: (a) piston displacement curve; (b) tracking error curves.

1 s–2 s period when the hydraulic cylinder piston transitions from rest to forward motion, both control methods exhibit transient errors, with TDAFSMC showing slightly larger initial errors compared to PID. However, during steady-state operation, the PID-controlled system displays sustained oscillations with approximately 0.35 mm error amplitude, which are attributed to system nonlinearities, including backlash, nonlinear friction, and other unmodeled dynamics. Prolonged exposure to these oscillations may lead to increased energy consumption, reduced operational stability, degraded precision, and potential equipment damage. In contrast, the TDAFSMC-controlled system maintains stable operation with only 0.16 mm steady-state error. During the 2 s–4 s interval, the PID-controlled system exhibits distinct limit cycle oscillations with sustained tracking errors averaging approximately 0.05 mm, while TDAFSMC achieves essentially zero error. When the piston reverses direction during 4 s–5 s, the PID-controlled system demonstrates 0.22 mm steady-state error compared to TDAFSMC's 0.15 mm. Overall, TDAFSMC improves tracking precision by 0.98 % across the complete operational cycle. These results confirm that the proposed TDAFSMC control strategy effectively enhances system stability, improves control accuracy, and significantly boosts the tracking performance of hydraulic systems by better compensating for nonlinear effects.

## 5. Experimental studies

To validate the controller's effectiveness and verify the simulation results, an experimental testbed for digital hydraulic cylinder position control was established, as illustrated in Fig. 7. Subsequent experiments were conducted to evaluate the system's response characteristics under various input signals. The main parameters of the digital hydraulic cylinder test platform are as follows: the variable vane oil pump of model VD1-30F-A3 has a displacement of 12 ml/r–40 ml/r, the motor of model CNS-2934/2.2 KW has a rotational speed of 1420 r/min, the control voltage of the West DAQ-Controller is ±10 V; and the MATLAB USB2.0 high data acquisition card has a rate of 38 Mb/s.

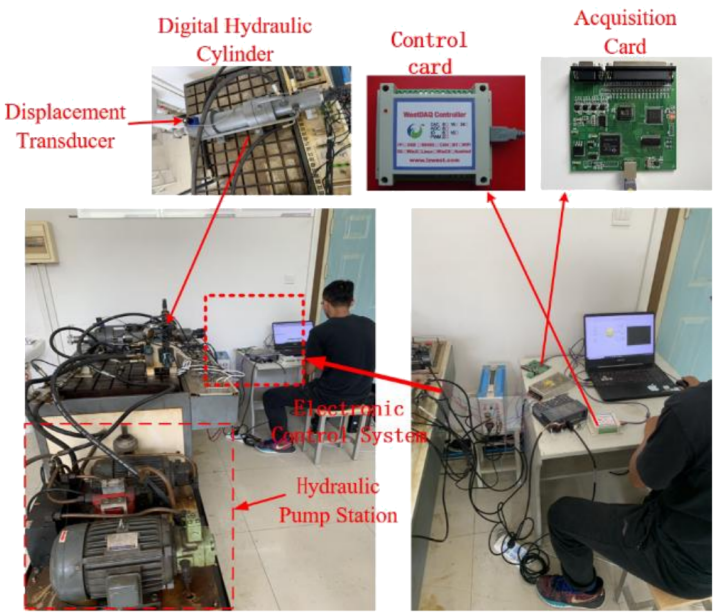


Fig. 7. Digital hydraulic cylinder position control system.

The digital hydraulic cylinder was operated under no-load conditions, with the relief valve in the hydraulic station functioning as a safety valve. The controller received the target displacement commands for piston rod 5 from the host computer 1. A wire-type displacement sensor acquired real-time position and velocity data during operation, which was transmitted

via a data acquisition card to provide feedback to the controller. Through the implemented control algorithm, the system achieved precise position control of the digital hydraulic cylinder.

To validate the control performance of the TDAMSFC strategy under real-world conditions, tracking experiments were conducted using the aforementioned three control signals. For step reference commands, Fig. 8 compares the tracking responses and errors under the different control strategies.

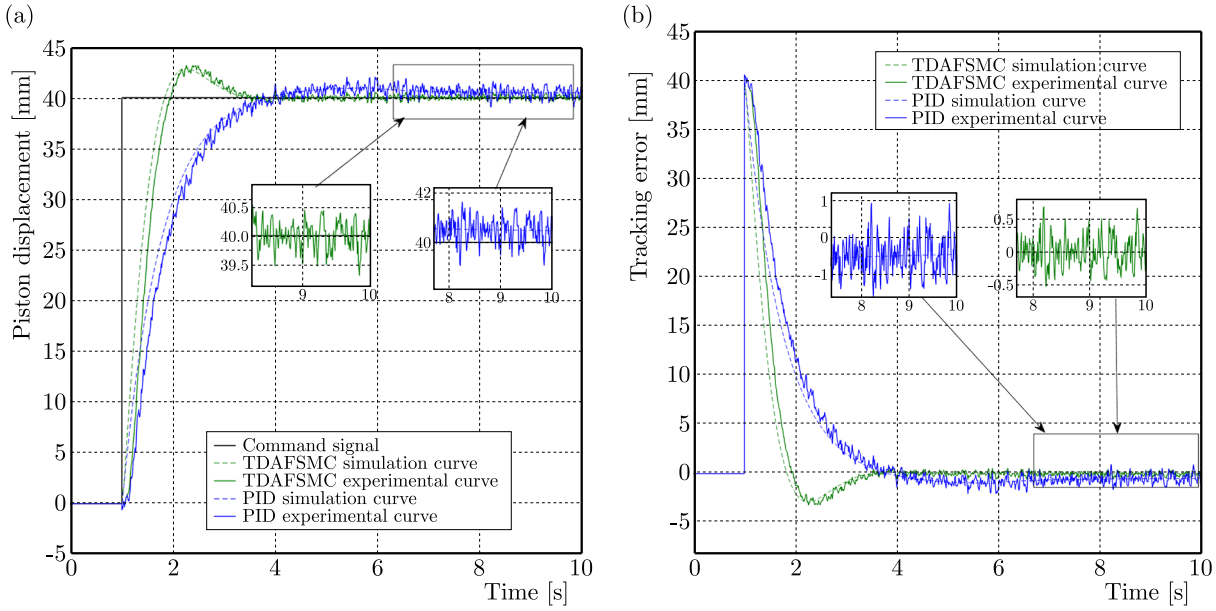


Fig. 8. Piston displacement and error curves: (a) piston displacement curve; (b) tracking error curves.

When reaching the target displacement, the PID-controlled system required approximately 6.5 s to stabilize, with ±1 mm deviation between the experimental and simulated trajectories. In contrast, the TDAMSFC-controlled system achieved stabilization in 3.3 s with only ±0.5 mm error, demonstrating a 49.2 % improvement in response speed and a 2.5 % enhancement in tracking accuracy. These experimental results confirm the superior transient performance and precision of the proposed TDAMSFC strategy, thereby verifying the theoretical analysis and simulation findings presented in this work.

Figure 9 presents the tracking responses and corresponding error profiles under sinusoidal reference commands for different control strategies. When tracking the target displacement, the PID-controlled system exhibits approximately 3 mm experimental error with a 2.1 mm deviation between the experimental and simulated trajectories, whereas the TDAMSFC-controlled system demonstrates superior performance with only 2 mm experimental error and 0.8 mm deviation between the experimental and simulated trajectories, representing a 3.25 % improvement in tracking accuracy. The magnified view in Fig. 9a further reveals that the TDAMSFC strategy significantly reduces the phase lag compared to PID control. These results confirm the enhanced tracking precision of the proposed TDAMSFC approach, providing additional validation for the theoretical and simulation analyses.

Figure 10 presents the tracking responses and corresponding error profiles under composite reference commands for different control strategies. When reaching the target displacement, the PID-controlled system requires approximately 3.0 s to stabilize with a 1.6 mm deviation between experimental and simulated trajectories, whereas the TDAMSFC-controlled system achieves stabilization in 2.6 s with only 1.4 mm deviation, demonstrating a 13.3 % improvement in response speed and a 0.5 % enhancement in tracking accuracy. These experimental results further validate that the proposed TDAMSFC strategy effectively improves control precision in practical applications.

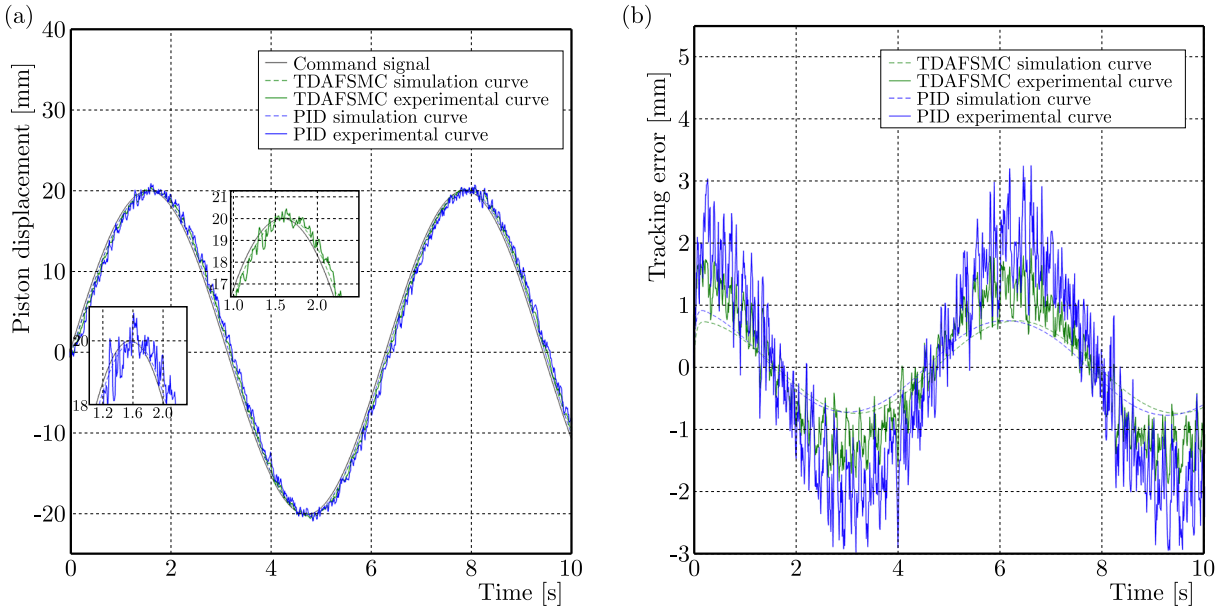


Fig. 9. Piston displacement and error curves: (a) piston displacement curve; (b) tracking error curves.

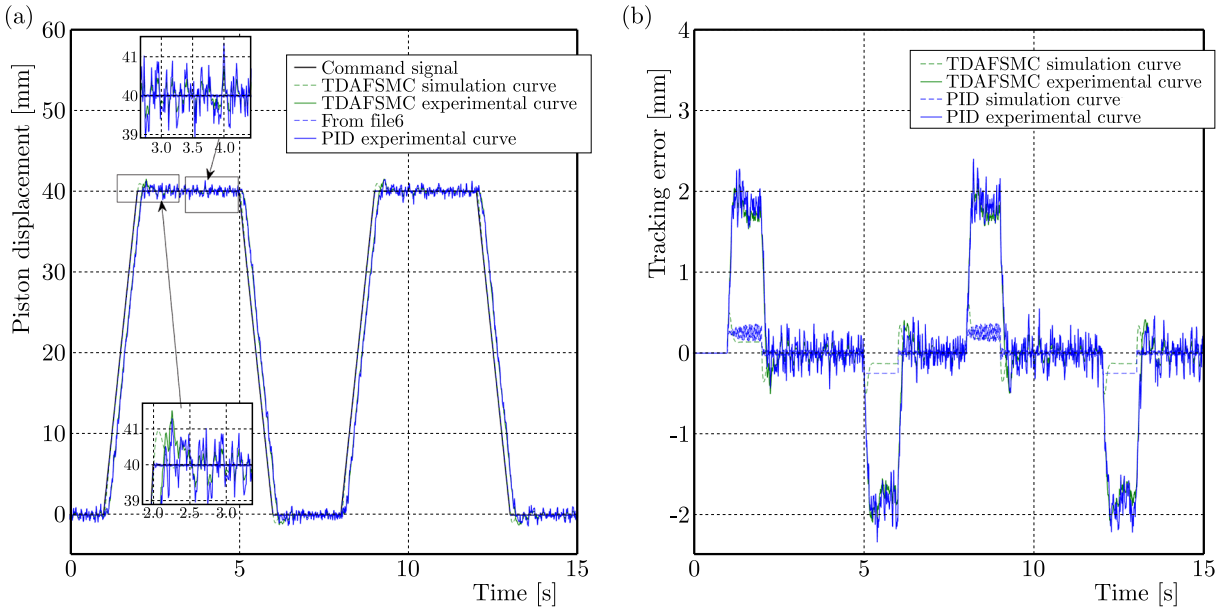


Fig. 10. Piston displacement and error curves: (a) piston displacement curve; (b) tracking error curves.

## 6. Conclusion

This study investigates output displacement tracking control for a digital hydraulic cylinder system characterized by nonlinear couplings such as clearance, hydrodynamic forces, and friction. By incorporating a TD, precise extraction of both the input signal and its differential information was achieved, significantly enhancing the perception of system dynamic characteristics. The TDAFSMC strategy was adopted, which utilizes a fuzzy system to approximate the switching term in sliding mode control, thereby ensuring controller continuity and effectively mitigating chattering. The stability and convergence of the closed-loop system were guaranteed via adaptive laws derived from Lyapunov theory.

A simulation model of the digital hydraulic cylinder position control system was constructed in the MATLAB/Simulink environment, and tests were conducted under various working con-

ditions, including step, sine, and composite signals. Simulation results demonstrate that under step response, the TDAFSMC strategy improved response speed by 41.7 % and reduced error by 2.0 % compared to traditional PID control. In sinusoidal tracking, both the phase lag and tracking error were significantly reduced. For composite signal tests, control accuracy was improved by 0.98 %. Experimental validation results were consistent with simulation trends, showing an average response error of less than 8.0 % and a tracking error below 1.0 %, fully confirming the superiority of the TDAFSMC strategy in terms of dynamic response, tracking accuracy, and disturbance rejection.

In conclusion, the proposed TDAFSMC method not only effectively enhances the control performance of digital hydraulic cylinder systems, exhibiting strong robustness and engineering applicability, but also provides a theoretical basis and technical support for the precise control of large-scale electro-hydraulic servo systems such as shearers and excavators. This study contributes positively to advancing control technology in high-end equipment systems.

## Acknowledgments

This research was supported by the National Natural Science Foundation of China (52204169) and the Heze University Doctoral Foundation (XY24BS04).

## References

1. Đào, T.L., & Thanh, L. (2023). Adaptive PID sliding mode controller application to position control of hydraulic system (in Vietnamese). *Journal of Transportation Science and Technology*, *12*(4), 26–33. https://doi.org/10.55228/jtst.12(4).26-33
2. Dang, X.J., Zhao, X.A., Dang, C., Jiang, H., Wu, X., & Zha, L. (2021). Incomplete differentiation-based improved adaptive backstepping integral sliding mode control for position control of hydraulic system. *ISA Transactions*, *109*, 199–217. https://doi.org/10.1016/j.isatra.2020.10.027
3. Gao, G., Zeng, Y., Liu, C., Wang, L., & Liu, R. (2023). Analysis of damping multi-mode switching control of semi-active suspension based on digital controlled hydraulic cylinders group. *Proceedings of the Institution of Mechanical Engineers, Part D: Journal of Automobile Engineering*, *239*(1), 98–112. https://doi.org/10.1177/09544070231210149
4. Ghani, M.F., Ghazali, R., Jaafar, H.I., & Soon, C.C. (2022). Real-time trajectory tracking control of an electro-hydraulic system using a fuzzy logic sliding mode controller. *2022 IEEE International Conference on Artificial Intelligence in Engineering and Technology (IICAIET)*, 1–6, https://doi.org/10.1109/iicaiet55139.2022.9936783
5. Guo, Y.-Q., Zha, X.-M., Shen, Y.-Y., Wang, Y.-N., & Chen, G. (2022). Research on PID position control of a hydraulic servo system based on Kalman genetic optimization. *Actuators*, *11*(6), Article 162. https://doi.org/10.3390/act11060162
6. He, J., Su, S., Wang, H., Chen, F., & Yin, B. (2023). Online PID tuning strategy for hydraulic servo control systems via SAC-based deep reinforcement learning. *Machines*, *11*(6), Article 593. https://doi.org/10.3390/machines11060593
7. Ji, X.H., Wang, C.W., Zhang, Z.Y., Chen, S., & Guo, X.P. (2021). Nonlinear adaptive position control of hydraulic servo system based on sliding mode back-stepping design method. *Proceedings of the Institution of Mechanical Engineers, Part I: Journal of Systems and Control Engineering*, *235*(4), 474–485. https://doi.org/10.1177/0959651820949663
8. Jiang, S.L., Wang, H., & Zhao, G.C. (2022). Research on neural network model reference adaptive disturbance rejection control of digital hydraulic cylinder. *Advances in Mechanical Engineering*, *14*(12). https://doi.org/10.1177/16878132221140706
9. Li, S., & Cao, X.H. (2021). Synchronous control characteristics analysis of shield propulsion hydraulic system based on tracking differentiator and self-adaptive PID. *International Journal of Pattern Recognition and Artificial Intelligence*, *35*(14), Article 2159053. https://doi.org/10.1142/s0218001421590539

10. Li, Z.B., Li, L., Zhang, J.Q., Huang, H.Y., & Sun, C.S. (2023). Nonsingular terminal sliding mode control of voice coil actuator fast steering mirror based on tracking differentiator. *2023 IEEE 18th Conference on Industrial Electronics and Applications (ICIEA)*, 1099–1105. https://doi.org/10.1109/iciea58696.2023.10241813

11. Liu, Y., Jiang, D., Yun, J., Sun, Y., Li, C., Jiang, G., Kong, J., Tao, B., & Fang, Z. (2022a). Self-tuning control of manipulator positioning based on fuzzy PID and PSO algorithm. *Frontiers in Bioengineering and Biotechnology*, *9*, Article 817723. https://doi.org/10.3389/fbioe.2021.817723

12. Liu, Y.J., Peng, X.W., Chen, X., & Guo, Y.J. (2022b). Electro-hydraulic proportional position control based on variable domain fuzzy PID. *2022 41st Chinese Control Conference (CCC)*, 2773–2778. https://doi.org/10.23919/ccc55666.2022.9902221

13. Qi, P.G., Chi, S., Zheng, Y.S., et al. (2024). Research on stiffness characteristics of 6-DOF parallel robot driven by digital hydraulic cylinder (in Chinese). *Journal of Ordnance Equipment Engineering*, *45*(6), 215–223. https://doi.org/10.11809/bqzbgcxb2024.06.030

14. Sun, C., Dong, X., Wang, M., & Li, J. (2022). Sliding mode control of electro-hydraulic position servo system based on adaptive reaching law. *Applied Sciences*, *12*(14), Article 6897. https://doi.org/10.3390/app12146897

15. Wang, L., Guan, S., Wu, Z., Wang, K., Li, Y., & Li, X. (2019). Design and simulation of intelligent lifting system based on digital hydraulic cylinder. *2019 IEEE 4th International Conference on Advanced Robotics and Mechatronics (ICARM)*, 24–29. https://doi.org/10.1109/icarm.2019.8833740

16. Yang, M.X., Zhang, Q., Lu, X.L., Xi, R., & Wang, X.S. (2019). Adaptive sliding mode control of a nonlinear electro-hydraulic servo system for position tracking. *Mechanika*, *25*(4), 283–290. https://doi.org/10.5755/j01.mech.25.4.22822

17. Yu, H., Wang, H., & Guo, C.G. (2024). Analysis of bandwidth expansion and interference suppression of digital hydraulic cylinder system. *International Journal of Control, Automation, and Systems*, *22*(5), 1739–1750. https://doi.org/10.1007/s12555-022-0589-3

18. Zhang, B., Niu, P., Guo, X., & He, J. (2024). Fuzzy PID control of permanent magnet synchronous motor electric steering engine by improved beetle antennae search algorithm. *Scientific Reports*, *14*, Article 2898. https://doi.org/10.1038/s41598-024-52600-8

19. Zhang, J.Z., & Fu, Y.J. (2025). Research on fluid motion characteristics of digital hydraulic cylinder control valve based on amesim and fluent. *Journal of Physics: Conference Series*, *3043*(1), Article 012046. https://doi.org/10.1088/1742-6596/3043/1/012046

20. Zhang, W., Xu, L., Liang, X., Zhang, Y., Yan, W., & Zhou, J. (2022). Position control of traction upper limb rehabilitation robot based on fuzzy sliding mode method. *2022 12th International Conference on CYBER Technology in Automation, Control, and Intelligent Systems (CYBER)*, 654–659. https://doi.org/10.1109/cyber55403.2022.9907696

*Manuscript received July 13, 2025; accepted for publication November 15, 2025; published online December 17, 2025.*